0026-895X/05/6804-983–994$20.00
MOLECULAR PHARMACOLOGY
Copyright © 2005 The American Society for Pharmacology and Experimental Therapeutics
Mol Pharmacol 68:983–994, 2005

Vol. 68, No. 4
11544/3054225
Printed in U.S.A.

MOL PHARM

MOLECULAR PHARMACOLOGY

Reactive Oxygen Species Elicit Apoptosis by Concurrently Disrupting Topoisomerase II and DNA-Dependent Protein Kinase

Hua-Rui Lu, Hong Zhu, Min Huang, Yi Chen, Yu-Jun Cai, Ze-Hong Miao, Jin-Sheng Zhang, and Jian Ding

Division of Anti-Tumor Pharmacology, State Key Laboratory of Drug Research, Shanghai Institute of Materia Medica*, Shanghai Institutes for Biological Sciences, Chinese Academy of Sciences, Shanghai, Peoples Republic of China (H.-R.L, H.Z., M.H., Y.C., Y.-J.C., Z.-H.M., J.-S.Z., J.D.); and Graduate School of the Chinese Academy of Sciences, Beijing, Peoples Republic of China (H.-R.L., H.Z., M.H.)*

Received January 28, 2005; accepted July 15, 2005

ABSTRACT

Reactive oxygen species (ROS) are produced by all aerobic cells and have been implicated in the regulation of diverse cellular functions, including intracellular signaling, transcription activation, proliferation, and apoptosis. Salvicine, a novel diterpenoid quinone compound, demonstrates a broad spectrum of antitumor activities. Although salvicine is known to trap the DNA-topoisomerase II (Topo II) complex and induce DNA double-strand breaks (DSBs), its precise antitumor mechanisms remain to be clarified. In this study, we investigated whether salvicine altered the levels of ROS in breast cancer MCF-7 cells and whether these ROS contributed to the observed antitumoral activity. Our data revealed that salvicine stimulated intracellular ROS production and subsequently elicited notable DSBs. The addition of *N*-acetyl cysteine (NAC), an antioxidant, effectively attenuated the salvicine-induced ROS enhancement and subsequent DNA DSBs. Heat treatment reversed the accumulation of DNA DSBs, and the addition of NAC attenuated the Topo II-DNA cleavable complexes formation and the growth inhibition of salvicine-treated JN394top2-4 yeast cells, collectively indicating that Topo II is a target of the salvicine-induced ROS. On the other hand, when examining the impact of salvicine on DNA repair pathways, we unexpectedly observed that salvicine selectively down-regulated the catalytic subunit of DNA-dependent protein kinase (DNA-PK_{CS}) protein levels and repressed DNA-PK kinase activity; both of these effects were attenuated by NAC pretreatment of MCF-7 cells. Finally and most importantly, NAC attenuated salvicine-induced apoptosis and cytotoxicity in MCF-7 cells. These results indicate that apart from its direct actions, salvicine generates ROS that modulate DNA damage and repair, contributing to the comprehensive biological consequences of salvicine treatment, such as DNA DSBs, apoptosis, and cytotoxicity in tumor cells. The finding of salvicine-induced ROS provides new evidence for the molecular mechanisms of this compound. Moreover, the effects of salvicine-induced ROS on Topo II and DNA-PK give new insights into the diverse biological activities of ROS.

Downloaded from molpharm.aspetjournals.org by guest on December 1, 2012

Reactive oxygen species (ROS; e.g., H_2O_2, hydroxyl radical, and superoxide anion) are traditionally regarded as toxic metabolic byproducts that have the potential to cause direct damage to biological macromolecules such as DNA. However, recent work has suggested that ROS plays a more widespread and exciting role as important signaling molecules. ROS may influence gene expression, cell proliferation, and cell death (Hancock et al., 2001). Low levels of ROS regulate cellular signaling and play important roles in normal cell proliferation (Kamata and Hirata, 1999). In some cases of apoptosis, ROS may be involved not only as inducers of DNA damage but also as specific messengers in the signal-trans-

This work was supported by grants from the National Natural Science Foundation of China (30330670), the Chinese Academy of Sciences (KSCX2-SW-202), and the Ministry of Science and Technology of China (2002AA2Z346A).

Article, publication date, and citation information can be found at http://molpharm.aspetjournals.org.

doi:10.1124/mol.105.011544.

ABBREVIATIONS: ROS, reactive oxygen species; Topo II, topoisomerase II; DSB, double-strand break; DNA-PK, DNA-dependent protein kinase; DNA-PKcs, catalytic subunit of DNA-PK; NAC, *N*-acetyl cysteine; DMSO, dimethyl sulfoxide; PBS, phosphate-buffered saline; DCF, 2,7-dichlorofluorescin; DCFH-DA, 2,7-dichlorodihydrofluorescein diacetate; TBE, Tris/borate/EDTA; DAPI, 4′,6-diamidino-2-phenylindole; PMSF, phenylmethylsulfonyl fluoride; SRB, sulforhodamine B; DTT, dithiothreitol; TUNEL, terminal deoxynucleotidyl transferase dUTP nick-end labeling; FITC, fluorescein isothiocyanate; NHEJ, nonhomologous end joining; HR, homologous recombination; PI, phosphatidylinositol; SN-38, 7-ethyl-10-hydroxycamptothecin.

duction pathway (Jabs, 1999; Higuchi, 2003; Haddad, 2004). ROS have also been implicated in the antitumor effects of some anticancer drugs (Sidoti-de Fraisse et al., 1998; Dai et al., 1999; Kotamraju et al., 2004; Yi et al., 2004). A number of anticancer drugs produce ROS at various cellular sites in vivo. Neocarzinostatin and bleomycin were shown to generate ROS in vivo and produce high molecular size (200~800 kilobases) DNA fragments and apoptotic internucleosomal DNA fragments during cell death. Cellular DNA cleavage into high-molecular-weight DNA fragments during apoptosis is highly reminiscent of topoisomerase II (Topo II)-mediated DNA cleavage in cells. Indeed, the patterns of DNA breaks induced by Topo II poisons are similar to those produced during apoptosis induced by other stimuli, such as ROS (Higuchi, 2003). However, the precise relationship between ROS and Topo II remains obscure.

Salvicine is a novel diterpenoid quinone compound synthesized by the structural modification of a natural product isolated from the Chinese medicinal herb *salvia prionitis lance* (Fig. 1). Salvicine possesses potent in vitro and in vivo activities against malignant tumor cells, particularly in some human solid tumor models (Qing et al., 1999), and induces apoptosis in various human tumor cell lines (Qing et al., 2001; Liu et al., 2002; Miao et al., 2003; Lu et al., 2005). It is noteworthy that salvicine shows prominent anti-multidrug resistance activities associated with down-regulation of mdr1 gene expression via the activation of c-jun (Miao and Ding, 2003; Miao et al., 2003). Mechanistic studies have shown that DNA Topo II is one of the primary molecular targets of salvicine (Meng et al., 2001a). Distinct from other classic Topo II inhibitors such as etoposide, salvicine acts on multiple steps of the Topo II catalytic cycle by promoting the binding of Topo II to DNA and inhibiting pre- and post-strand–mediated DNA religation without impacting the forward cleavage steps. This suggests that salvicine might promote DNA strand breaks by stabilizing the cleavable complex (Meng et al., 2001b). Further work in human breast carcinoma MCF-7 cells demonstrated that salvicine was responsible for inducing DNA double-strand breaks (DSBs), which have been proposed to be responsible for cell death (Lu et al., 2005).

Accumulating evidence has suggested that the molecular mechanisms of salvicine activity in tumor cells may be complex. Salvicine structurally contains quinone, a chemically active moiety. Most of the quinone-containing anticancer drugs are believed to stimulate ROS as part of their antitumor activities or important toxicities (Shiah et al., 1999; Minotti et al., 2001; Wang et al., 2001; Kotamraju et al., 2004). However, the detailed mechanisms and cellular responses of salvicine-induced DNA damage are not yet well understood. Here, we investigated whether salvicine alters the levels of ROS in breast cancer MCF-7 cells, analyzed the roles of ROS in salvicine-induced DNA damage and repair responses, and determined the contribution of ROS to the antitumor activity of salvicine.

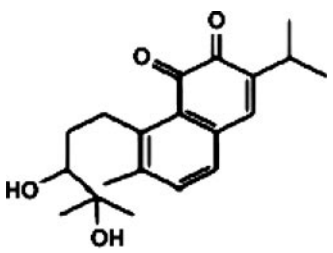

Fig. 1. Chemical structure of salvicine.

Materials and Methods

Drugs and Reagents. Tangerine yellow crystalloid salvicine was kindly provided by Professor Jin-Sheng Zhang from the Department of Phytochemistry in the Shanghai Institute of *Materia Medica*. Salvicine (65% yield) was purified by column chromatography on silica gel eluted with a cyclohexane-ethyl acetate mixture (4:1, v/v). Its purity was greater than 99.8%, as determined by high-performance liquid chromatography (Zhang et al., 1999). The compound was solubilized at a concentration of 10 mM in dimethyl sulfoxide (DMSO) as stock solution and was stored at −20°C in the dark. Aliquots were thawed just before each experiment and diluted to the desired concentrations with normal saline. *N*-acetyl-cysteine (NAC) (Sigma Chemical, St. Louis, MO) was diluted to 600 mM in phosphate-buffered saline (PBS) and stored at 4°C, whereas 2,7-dichlorodihydrofluorescein diacetate (DCFH-DA) (Sigma) was diluted to 25 mM in DMSO and stored at −20°C. The final DMSO concentration did not exceed 0.1%. Other reagents were of analytical grade.

Cell Culture. The human breast carcinoma cell line, MCF-7, was obtained from the American Type Culture Collection (Manassas, VA). Cells were maintained as a monolayer culture in RPMI 1640 medium (Invitrogen, Grand Island, NY) containing 10% (v/v) heat-inactivated fetal bovine serum, 2 mM glutamine, 100 U/ml penicillin, 100 μg/ml streptomycin, and 1 mM sodium pyruvate, supplemented with 0.01 mg/ml bovine insulin (Sigma) under a humidified atmosphere containing 5% CO_2 at 37°C.

Yeast Strain. The *Saccharomyces cerevisiae* strain JN394top2-4, in which the wild-type Topo II gene was replaced with the temperature-sensitive top2–4 mutant allele (Binaschi et al., 1998), was the generous gift of Dr. Neil Osheroff (School of Medicine, Vanderbilt University, Nashville, TN). Yeasts were grown in liquid medium (1% yeast extract, 2% bactopeptone, 2% glucose, and 40 μg/ml adenine) at 25 or 35°C.

ROS Detection. Cellular ROS levels were quantified as described previously (Yi et al., 2004). Accumulation of intracellular ROS was detected with DCFH-DA, which crosses cell membranes and is hydrolyzed by intracellular nonspecific esterases to nonfluorescent DCFH. In the presence of ROS, DCFH is oxidized to highly fluorescent DCF, which is readily detected by flow cytometry. The DCF fluorescence intensity is proportional to the amount of intracellularly formed ROS (LeBel et al., 1992).

MCF-7 cells were seeded into six-well plates at a density of 5×10^5/ml, cultured overnight, and then incubated with different concentrations of salvicine at 37°C for the indicated times. Before harvesting, cells were incubated with DAFH-DA (final concentration, 10 μM) for 15 min. Where noted, NAC (5 mM), when used, was preincubated for 1 h with cells. Cells were washed with ice-cold PBS, pH 7.4, collected, and kept on ice in the dark for immediate detection with a flow cytometer (FACSCalibur; BD Biosciences, San Jose, CA).

The levels of ROS in yeast JN394top2-4 cultured under two different temperatures (25 and 35°C) were detected using the above-mentioned procedures with the following modifications: cells were exposed to the various concentrations of salvicine for 1 h, and the pretreatments with DCFH-DA (0.1 mM) and NAC (10 mM) lasted 1 and 2 h, respectively.

Neutral Single-Cell Gel Electrophoresis Assay. DNA DSBs were evaluated using the neutral single-cell gel electrophoresis assay (the neutral comet assay), as described previously (Olive et al., 1990) with minor modifications (Lu et al., 2005). In brief, MCF-7 cells (5×10^5/ml) were seeded into six-well plates, incubated overnight, and then treated with various concentrations of salvicine for the indicated times. The samples were left untreated or were pretreated

MOL PHARM
MOLECULAR PHARMACOLOGY
aspet
Downloaded from molpharm.aspetjournals.org by guest on December 1, 2012

MOL PHARM

MOLECULAR PHARMACOLOGY

with NAC (5 mM) for 1 h before salvicine addition. Cells were harvested and resuspended in ice-cold PBS at 5×10^5/ml. Cells (25 μl) were mixed with an equal volume of 1% low-melting-point agarose, layered onto microscope slides precoated with 50 μl of 1% normal-melting-point agarose, and spread gently with a coverslip to avoid creating bubbles. The agarose was allowed to solidify for 10 min at 4°C, the coverslip was carefully removed, and the slides were immersed in ice-cold fresh lysis solution (2.5 M NaCl, 100 mM Na_2EDTA, 10 mM Tris, 10% DMSO, 1% Triton X-100, and 1% laurosylsarcosinate) for 80 min at 4°C in a dark chamber. After lysis, the slides were equilibrated for 20 min with TBE buffer (90 mM Tris, 90 mM boric acid, and 2 mM EDTA, pH 8.0), and electrophoresis was performed in TBE buffer at 30 V, 15 mA for 20 min. After electrophoresis, the slides were dried at room temperature for 5 to 10 min, and then 20 μl of 4′,6-diamidino-2-phenylindole (DAPI, 1 μg/ml in PBS) was pipetted onto the agarose surface under a coverslip. Individual cells were viewed using a UV light fluorescence microscope (BX51; Olympus, Tokyo, Japan). Quantification was achieved by analyzing at least 50 randomly selected comets per slide with the Komet 5.5 software (Kinetic Imaging Ltd., Nottingham, UK) using the following parameters: tail length (estimated leading edge from the nucleus; in micrometers), L/H (the ratio of tail length to head diameter), and tail moment (arbitrary units; defined as the product of the percentage of DNA in the tail multiplied by the tail length). In heat-induced reversal experiments, cells were heated to 55°C for 10 min before lysis.

Trapped in Agarose DNA Immunostaining Assay. The Topo II-DNA cleavable complexes were examined using the trapped in agarose DNA immunostaining (TARDIS) assay as reported previously (Willmore et al., 1998). In brief, untreated or treated MCF-7 cells were harvested and mixed with low-melting gel spreading on slides, followed by placing the slides in lysis buffer containing protease inhibitors for 30 min at 20°C. The lysis buffer contained 1% SDS, 80 mM phosphate buffer, pH 6.8, 10 mM EDTA, and a protease inhibitor mixture (2 μg/ml pepstatin A, 2 μg/ml leupeptin, 1 mM PMSF, and 1 mM dithiothreitol). Slides were next immersed in 1 M NaCl supplemented with the protease inhibitor mixture for 30 min and then washed by immersion three times in PBS. Then, 1 M NaCl removed proteins that were not covalently bound to the DNA. Topo II that covalently bound to the DNA of each cells was detected using topo IIα-specific rabbit polyclonal antibody (Santa Cruz Biotechnology, Santa Cruz, CA) and Alexa Fluor 488 goat anti-rabbit IgG (Molecular Probes, Eugene, OR). DNA was stained with DAPI (1 μg/μl). Image was captured using fluorescence microscope (BX51, Olympus).

Sulforhodamine B Dye Assay. The cytotoxicity of salvicine against MCF-7 cells was evaluated by sulforhodamine B (SRB) dye assay, as described previously (Lu et al., 2005). In brief, 100 μl of cells (5×10^4/ml) per well were seeded in 96-well plates. Cells were treated in triplicate with gradient concentrations of salvicine for 72 h at 37°C, and where appropriate, samples were pretreated with NAC (5 mM) for 1 h. At the end of exposure, cells were fixed, washed, dried, and stained with SRB (Sigma). The bound stain was solubilized with Tris buffer, and optical density was measured at 515 nm using a multiwell spectrophotometer (VERSAmax; Molecular Devices, Sunnyvale, CA). The growth inhibition rate was calculated by the following equation: growth inhibition rate = $[1 - (A_{515\ treated}/A_{515\ control})] \times 100\%$.

Microwell Assay. The effect of NAC on the growth inhibition of yeast JN394top2-4 cells by salvicine was determined by a microwell assay described previously (Hammonds et al., 1998). Yeast strain JN394top2-4 was seeded in 96-well microplates (5×10^5 and 1×10^6 cells/ml, 180 μl/well) and cultured at 25 and 35°C, respectively. Cells were treated in triplicate with gradient concentrations of salvicine for 24 h at 25 and 35°C, respectively. For experiments, samples were preincubated with NAC (10 mM) for 2 h before the addition of salvicine. Optical density was measured at 630 nm with a multiwell spectrophotometer. The results were expressed as the relative survival rate, which was calculated as $(OD_{control} - OD_{treated})/OD_{control} \times 100\%$.

DNA-Dependent Protein Kinase Activity Assay. Exponentially growing MCF-7 cells were treated with various concentrations of salvicine and with or without 1-h preincubation with 5 mM NAC for the required periods, and whole-cell extracts were prepared as described previously (Eriksson et al., 2001). In brief, cells were washed with ice-cold PBS, pH 7.4, trypsinized, and then washed twice with ice-cold PBS. Samples were then lysed in low-salt buffer (10 mM HEPES, pH 7.6, 25 mM KCl, 10 mM NaCl, 2 mM $MgCl_2$, 0.1 mM EDTA, 1 mM DTT, 0.1 mM PMSF, and 5 μl of Protease Inhibitor Cocktail per milliliter of lysis buffer) in a volume equal to three times the cell pellet volume and incubated on ice for 20 min. The lysates were centrifuged at 10,000*g* for 10 min at 4°C. Supernatants were collected, and the insoluble material was treated with a high-salt buffer (10 mM HEPES pH 7.6, 25 mM KCl, 0.4 M NaCl, 2 mM $MgCl_2$, 0.1 mM EDTA, 1 mM DTT, 0.1 mM PMSF, and 5 μl of Protease Inhibitor Cocktail per milliliter of lysis buffer), incubated on ice for 20 min, and pelleted at 10,000*g* for 10 min at 4°C. Supernatants obtained from the high-salt extraction were pooled with the supernatants from the low-salt extraction. Total protein concentration was quantified using the BCA method (Micro BCA Protein Assay Reagent Kit; Pierce Chemical, Rockford, IL).

DNA-dependent protein kinase (DNA-PK) activity was determined by a DNA-PK assay system (SignaTECT DNA-Dependent Protein Kinase Assay System; Promega, Madison, WI) according to the manufacturer's instructions with minor modifications. In brief, 0.4 mM biotinylated peptide substrate in a reaction buffer containing 50 mM HEPES, pH 7.5, 100 mM KCl, 10 mM $MgCl_2$, 0.1 mM EDTA, 0.2 mM EGTA, 1 mM DTT, 0.1 mM ATP, and 0.5 μCi of [γ-^{32}P]ATP was added to a DNA-PK activation buffer (0.25 μg of calf thymus) or a control buffer (1 mM Tris-HCl, pH 7.4, and 0.1 mM EDTA, pH 8.0) and preincubated at 30°C for 5 min. Reactions were then initiated by adding 12.5 μg of cellular protein per assay. The final volume was adjusted to 25 μl with deionized water, and reactions were incubated at 30°C for 8 min. Reactions were stopped with 12.5 μl of termination buffer (2.5 M guanidine hydrochloride) and spotted onto SAM^2 Biotin Capture Membranes (Promega). Membranes were then washed in 2 M NaCl, washed in 2 M NaCl in 1% H_3PO_4, and finally washed in deionized water. Radioactivity was defined as the counts per minute of ^{32}P incorporated in the presence of DNA minus the counts per minute of ^{32}P incorporated in the absence of DNA. The DNA-PK activity was calculated as described in the kit protocol.

Western Blot Analysis. MCF-7 cells ($1.2\sim1.5 \times 10^6$/ml) were seeded into 60-mm culture dishes and treated with salvicine alone or combined with NAC for the desired periods. Cells were washed twice with ice-cold PBS and then lysed in lysis buffer (2 mM sodium orthovanadate, 50 mM NaF, 20 mM HEPES, pH 7.5, 150 mM NaCl, 1.5 mM $MgCl_2$, 5 mM sodium pyrophosphate, 10% glycerol, 0.2% Triton X-100, 5 mM EDTA, 1 mM PMSF, 10 μg/ml leupeptin, and 10 μg/ml aprotinin) on ice for 30 min. Insoluble materials were pelleted at 13,000*g* for 20 min at 4°C. Equal amounts of protein (50 μg for the analysis of DNA-PKcs, 20 μg for others) were electrophoresed on 6% (for DNA-PKcs) or 10% (for Ku70, Ku86, Mre11, and Rad51) SDS polyacrylamide gels. Then, proteins were electroblotted onto nitrocellulose membranes and identified with mouse monoclonal antibodies at dilutions of 1:1000 for DNA-PKcs, 1:1000 for Ku70, and 1:1000 for Ku86; rabbit polyclonal antibody at 1:1000 dilution for Rad51, or goat polyclonal antibodies at 1:500 and 1:1000 dilution for Mre11 and β-actin, respectively (all from Santa Cruz Biochemicals, Santa Cruz, CA). The bound primary antibodies were reacted with the appropriate anti-mouse (1:1000), anti-rabbit (1:1000), or anti-goat (1:1000) horseradish peroxidase-labeled secondary antibodies, and the results were visualized by enhanced chemiluminescence (Pierce Chemical) according to the manufacturer's instructions.

Apoptosis Assessment. Cells (5×10^5) were exposed to various concentrations of salvicine for 24 h with or without 5 mM NAC pretreatment (1 h). The apoptotic cell fraction in salvicine-treated

Downloaded from molpharm.aspetjournals.org by guest on December 1, 2012

MCF-7 cells was assessed by two independent methods. DNA fragmentation was examined by terminal deoxynucleotidyl transferase dUTP nick-end labeling (TUNEL) with an in situ fluorescein-based cell death detection kit (Roche Diagnostics, Mannheim, Germany). Cells were washed, fixed, stained, and digitally photographed under a fluorescence microscope (Olympus BX51) according to the manufacturer's protocol. Quantification of apoptotic MCF-7 cells was performed with an Annexin V-FITC apoptosis detection kit (BD Biosciences) according to the manufacturer's instructions. At least 10,000 cells from each sample were examined using a FACSCalibur Analyzer (BD Biosciences). Experiments were repeated twice.

Immunocytochemical Analysis. MCF-7 cells (5×10^4/ml, 1 ml/well) plated on coverslips in 24-well plates were used to study the subcellular localization of DNA-PK (Ku70, Ku86, and DNA-PKcs). Mock- and drug-treated cells were air-dried, fixed for 30 min with 4% paraformaldehyde in PBS, pH 7.4, at room temperature, and washed twice with PBS. Then, the cells were incubated for 10 min with 0.2% Triton X-100 and washed with PBS. After that, the cells were incubated with blocking buffer (3% bovine serum albumin in PBS) for 30 min at room temperature before being incubated for 1 h with primary antibodies to DNA-PKcs, Ku70, or Ku86 (1:500; Santa Cruz Biochemicals). After three washes (10 min each) with PBS, the cells were incubated for 1 h at room temperature with the Alexa488-conjugated secondary antibody (1:250; Alexa Fluor 488 goat anti-mouse IgG, Molecular Probes). The cells were washed three times and stained with 0.5 μg/ml DAPI for 30 min in the dark. Images were

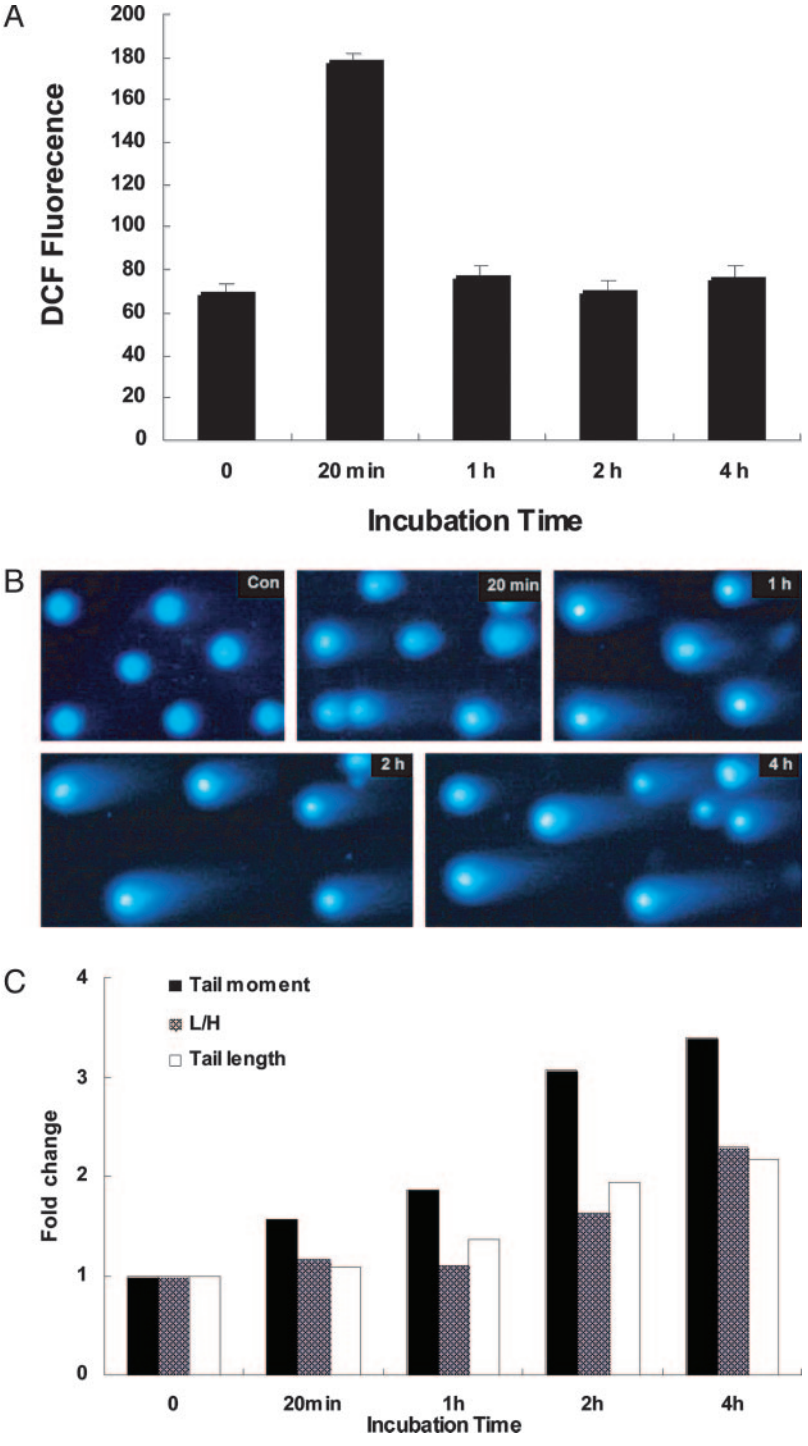

Fig. 2. Effects of salvicine on intracellular ROS levels and DNA integrity. MCF-7 cells were treated with 20 μM salvicine and harvested at the indicated time points. ROS levels were detected by flow cytometry using a DCFH-DA fluorescent probe; results are expressed as DCF fluorescence intensity. DNA double-strand breaks were determined by the neutral comet assay and were semiquantified using the Komet 5.5 software. A, kinetics of ROS production in MCF-7 cells after salvicine treatment. Each data point (mean ± S.D.) represents the mean fluorescence of 10,000 cells from two independent experiments. B, the morphological appearance of MCF-7 cells after neutral electrophoresis (200×). C, semiquantitative analysis of the results in B expressed as fold change of the following parameters: tail moment, L/H, and tail length.

MOL PHARM
MOLECULAR PHARMACOLOGY
aspet
Downloaded from molpharm.aspetjournals.org by guest on December 1, 2012

photographed using a Leica TCS Confocal Microscope (Leica Microsystems, Inc., Deerfield, IL).

Results

Salvicine Increases Intracellular ROS Levels before Induction of DNA DSBs. We investigated the effect of salvicine on intracellular ROS and DNA integrity. MCF-7 cells were exposed to salvicine and harvested at various time points. The intracellular ROS levels were detected by flow cytometry using DCFH-DA fluorescent probes, and DSBs were evaluated by neutral single-cell gel electrophoresis (also called the comet assay). In salvicine-treated MCF-7 cells, the cellular ROS levels experienced a rapid increase after treatment and then rapidly decreased back to basal levels, whereas DNA DSBs showed a delayed onset followed by a gradual, steady increase (Fig. 2). After 20-min treatment of MCF-7 cells with 20 μM salvicine, the DCF fluorescence intensity (corresponding to the intracellular ROS levels) increased up to 2.6 times the basal value (Fig. 2A). At this time, images from the comet assay showed no obvious "comet tails", which represent the degree of cellular DNA DSBs. There were only obscure "halos" around the individual nuclei, and the tails had no clear direction (Fig. 2B). The ROS levels returned to basal values after 1 h and maintained basal levels thereafter. In striking contrast, the degree of cellular DNA DSBs increased with treatment time, as evidenced by the frequent appearance and expanding volume of comet tails with corresponding shrinkage of the comet heads. Semiquantitative analysis with the Komet 5.5 software confirmed these observations and revealed that 4 h after treatment, the DNA damage degree reached more than two to three times that of the control (Fig. 2C). In view of the active nature of

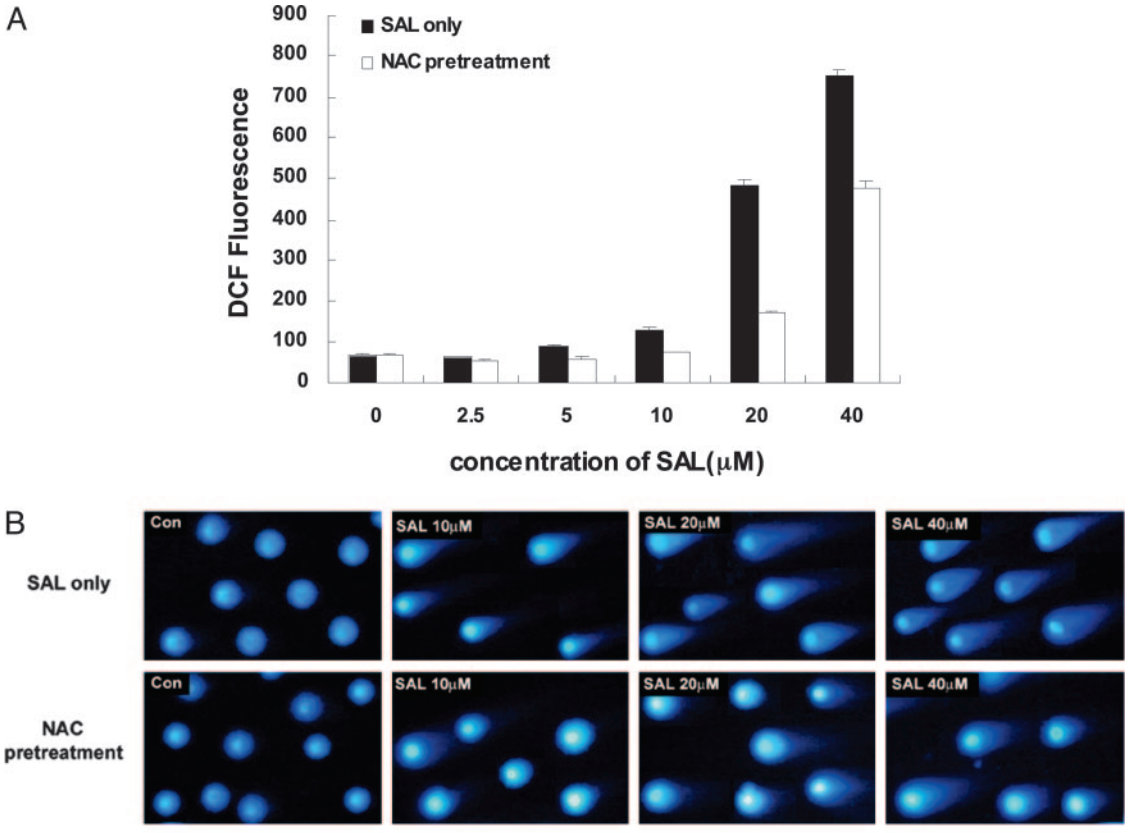

C

Concentration(μM)	Tail moment		L/H		Tail length	
	SAL only	NAC pretreatment	SAL only	NAC pretreatment	SAL only	NAC pretreatment
0	2.44±2.25	2.01±1.69	1.10±0.36	0.96±0.77	14.53±10.44	15.25±11.91
2.5	3.87±2.17	2.88±0.94	1.08±0.38	1.57±0.09	24.57±8.15	23.05±5.61
5	5.22±2.10	2.53±0.71	1.63±0.49	1.39±0.13	33.70±9.43	20.99±3.66
10	7.41±0.61	2.97±0.99	2.20±0.31	1.50±0.10	44.67±2.54	27.17±6.18
20	9.13±2.29	3.76±1.28	2.35±0.44	1.80±0.38	49.67±7.74	30.11±7.75
40	9.98±2.77	4.10±1.86	2.90±0.43	1.51±0.37	57.77±4.47	29.15±9.08

Fig. 3. Effects of NAC pretreatment on ROS levels and DNA double-strand breaks. MCF-7 cells were exposed to gradient concentrations of salvicine with or without pretreatment with 5 mM NAC for 1 h. A, NAC pretreatment reduced ROS production after 20-min salvicine treatment. B, the protective effect of NAC on salvicine-induced DSBs (200×). C, semiquantitative analysis of the results presented in B expressed as mean ± S.D. (n = 3).

MOL PHARM
MOLECULAR PHARMACOLOGY
aspet
Downloaded from molpharm.aspetjournals.org by guest on December 1, 2012

ROS, these results suggest that ROS might contribute to salvicine-induced DNA DSBs but may not directly affect DNA.

NAC Attenuates Salvicine-Induced ROS Enhancement and Subsequent DNA DSBs. NAC is an ROS scavenger that has been widely used to define the role of ROS in numerous biological and pathological processes (Zafarullah et al., 2003). To clarify the relationship between salvicine-induced cellular ROS enhancement and DNA DSBs, we used NAC to examine the effects of intracellular ROS depletion on salvicine-induced DSBs. MCF-7 cells were exposed to gradient concentrations of salvicine for 20 min with or without 5 mM NAC. In the range of 2.5 to 40 μM, salvicine was found to elevate intracellular ROS levels in a dose-dependent manner, and pretreatment with 5 mM NAC diminished the salvicine-induced elevation of ROS levels (Fig. 3A). The correlation between increased ROS levels and salvicine-induced DSBs was analyzed by pretreatment of samples with 5 mM

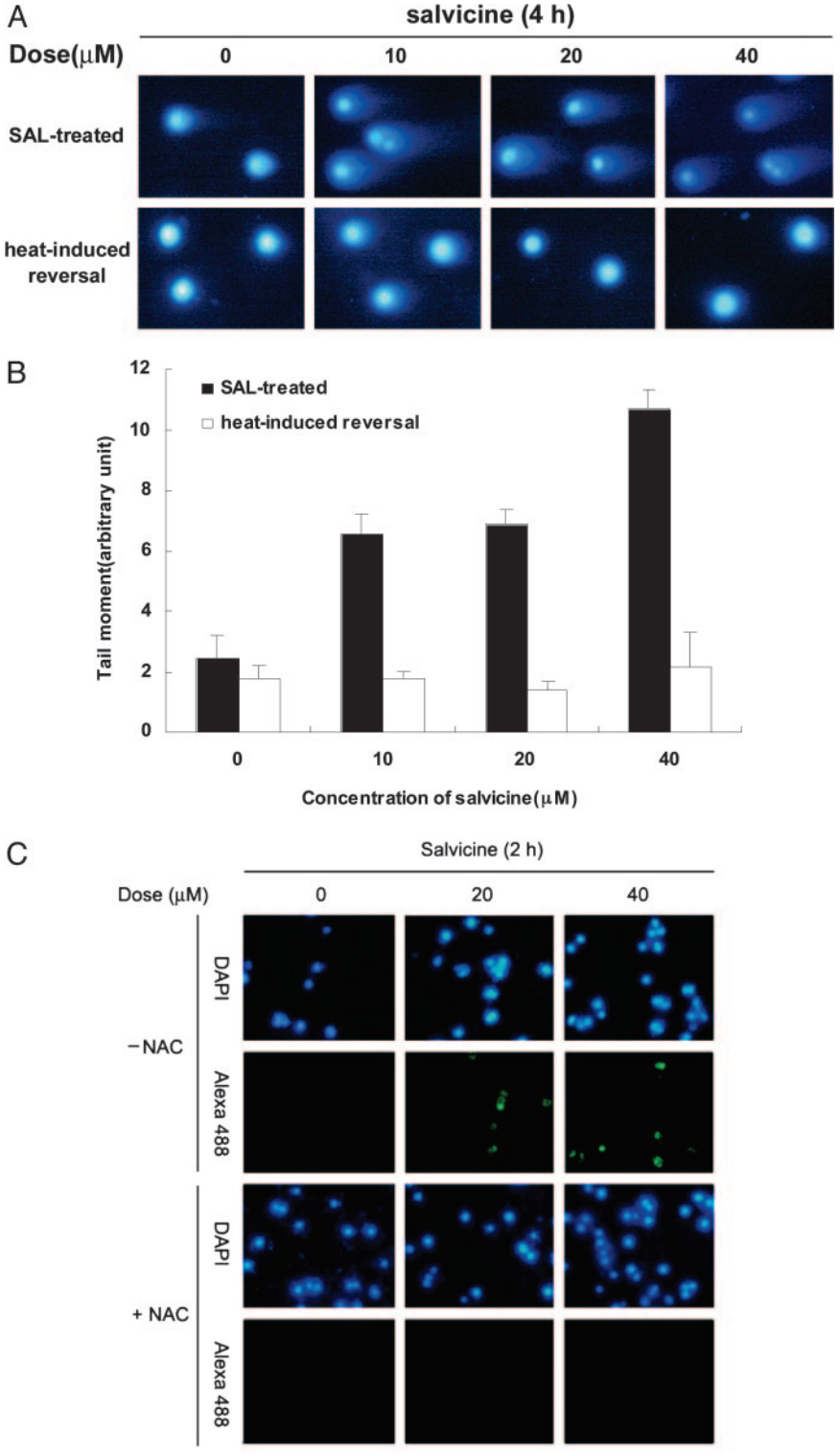

Fig. 4. Salvicine induces Topo II-DNA–cleavable complexes and reversible DNA DSBs. MCF-7 cells were treated with salvicine as indicated, and a neutral comet assay was performed to analyze the DNA integrity. Reversal of DNA DSBs was examined by shifting the treated cells to 55°C for 10 min before lysis. The formation of complexes was examined by TARDIS assay as described under *Materials and Methods.* A, representative comet images are shown (200×). B, semiquantitative analysis of the results presented in A expressed as Olive tail moment (mean ± S.D., $n = 3$). C, representative immunofluorescence image of TARDIS.

MOL PHARM
MOLECULAR PHARMACOLOGY
aspet
Downloaded from molpharm.aspetjournals.org by guest on December 1, 2012

NAC before the addition of salvicine. As seen in the representative images of the comet assay (Fig. 3B), NAC prominently protected cells from salvicine-induced DSBs. The protective effect of NAC was reflected more clearly by the semiquantitative analysis, which revealed that the parameters (tail moment, tail length, and L/H) in NAC-pretreated groups all displayed decreasing trends compared with salvicine-treated groups (Fig. 3C). Thus, NAC not only attenuated the increased ROS levels induced by salvicine but also inhibited the DSBs elicited by salvicine. These results indicate that ROS play causative roles in salvicine-induced DNA damage in MCF-7 cells.

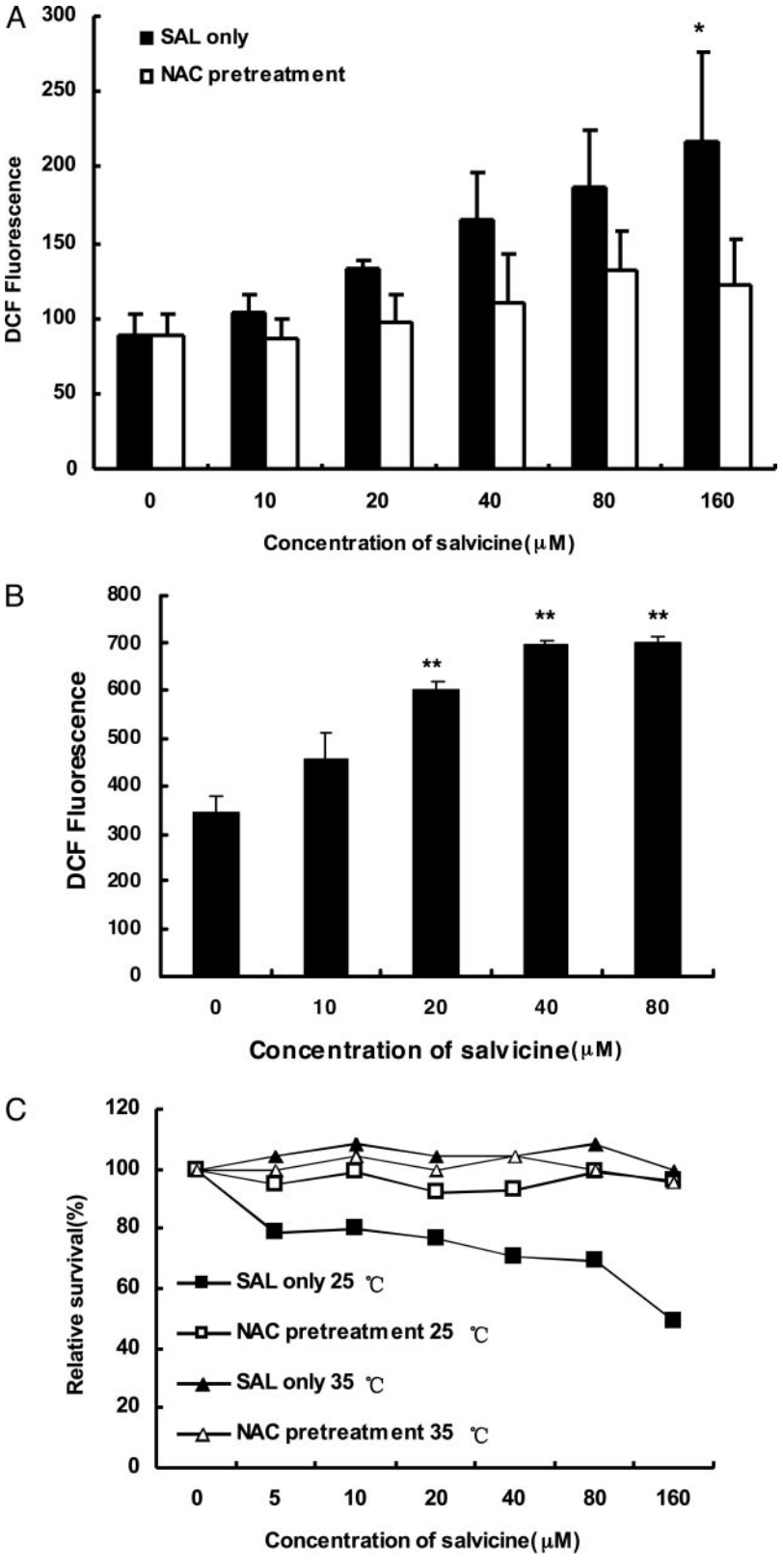

Fig. 5. Effect of NAC on salvicine-induced ROS enhancement and growth inhibition in JN394top2-4 at different incubation temperatures. JN394top2-4 cells were treated as described under *Materials and Methods*. ROS levels were detected with the DCFH-DA probe, and growth inhibition was evaluated by the microwell assay. A, salvicine elevated the intracellular ROS levels in JN394top2-4 cells cultured at 25°C; this effect was reversed by NAC pretreatment. B, salvicine also elevated the intracellular ROS levels in JN394top2-4 at 35°C. C, NAC attenuates the growth inhibition by salvicine in JN394top2-4 cells at 25 but not at 35°C. The data are expressed as the relative survival (shown as a percentage) from three independent experiments. The significance was assessed with analysis of variance. ⋆, $p < 0.05$, ⋆⋆, $p < 0.01$ compared with 0 μM salvicine.

MOL PHARM
MOLECULAR PHARMACOLOGY
aspet
Downloaded from molpharm.aspetjournals.org by guest on December 1, 2012

MOL PHARM
MOLECULAR PHARMACOLOGY
aspet

Salvicine-Induced DSBs Are Caused by the Formation of Topo II-DNA Cleavable Complexes. In the present study, salvicine stimulated intracellular ROS levels and subsequent damage to DNA duplexes. ROS can directly react with biological molecules such as DNA or may indirectly act as signaling molecules. Thus, we next sought to distinguish between these two possible actions of ROS in salvicine-induced DNA DSBs. Heat-induced reversibility is a unique property of Topo II-cleavable complexes (Hsiang and Liu, 1989). When salvicine-treated MCF-7 cells were heated to 55°C for 10 min before lysis, the salvicine-induced DNA DSBs disappeared completely (Fig. 4, A and B), indicating that the salvicine-induced DSBs were caused by the formation of Topo II-cleavable complexes rather than by random DNA breakage. Furthermore, we directly measured Topo II-DNA cleavable complex formation using the TARDIS assay, a novel immunofluorescence technique in situ, to confirm the hypothesis. As expected, we found that the Topo II-cleavable complexes were formed in MCF-7 cells treated with 20 or 40 μM salvicine, and NAC (5 mM) pretreatment effectively inhibited salvicine-induced the formation of Topo II-cleavable complexes (Fig. 4C). By integrating these data, we note that NAC not only attenuated the salvicine-induced DSBs but also inhibited the formation of Topo II-DNA cleavable complexes, indicating that salvicine-mediated ROS production might act as signaling molecules to mediate DNA damage through the function of Topo II.

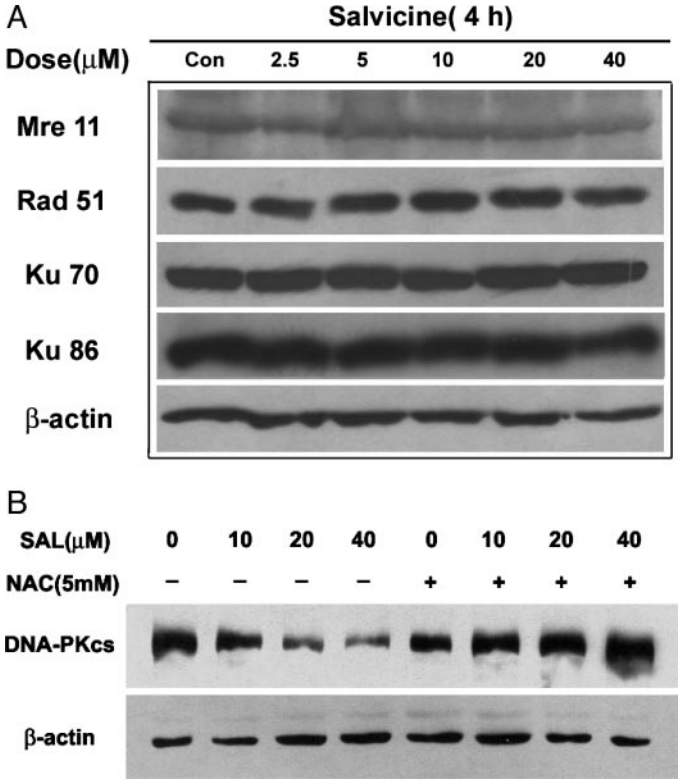

Fig. 6. NAC reverses the salvicine-induced down-regulation of DNA-PKcs protein levels. Cells were treated and detected as indicated under *Materials and Methods*. The experiments were repeated at least three times. A, effects of salvicine on the expression of various proteins. B, effects of NAC pretreatment on DNA-PKcs expression.

Topo II Is One Target of Salvicine-Induced ROS. Because we showed that Topo II is one of the main targets of salvicine, we further examined whether salvicine-induced ROS affected Topo II to elicit the observed biological effects. The yeast strain JN394top2-4 contains a Topo II temperature-sensitive mutation that alters Topo II activity in the yeast strain according to the culture temperature. At 25°C, the yeast has full wild-type Topo II enzyme activity, but this activity is completely abrogated at 35°C. Salvicine elevated the intracellular ROS levels in JN394top2-4 in a dose-dependent manner at 25°C, and this was reversed by NAC pretreatment (Fig. 5A). The same augmentation of ROS levels was observed at 35°C (Fig. 5B). NAC pretreatment reversed the growth inhibition of salvicine on JN394top2-4 at 25°C

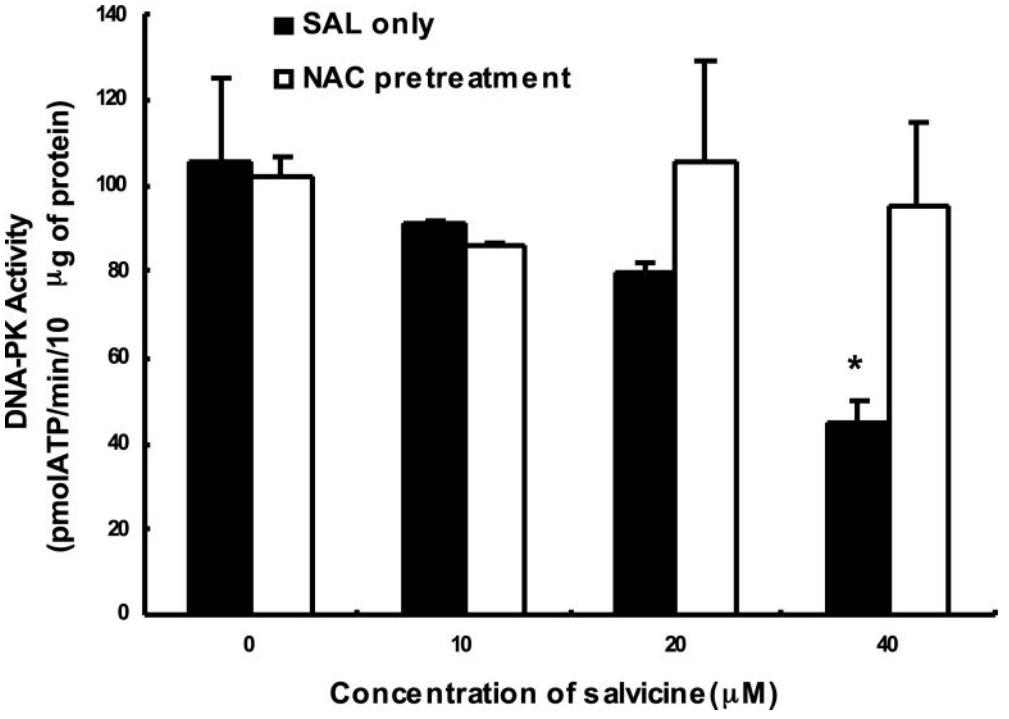

Fig. 7. Effect of salvicine on DNA-PK activity. Salvicine inhibited the activity of DNA-PK extracted from drug-treated cells, and NAC pretreatment reversed the inhibition of DNA-PK. The mean ± S.D. values of three independent experiments are shown. The significance was assessed with analysis of variance. ⋆, $p < 0.05$ compared with 0 μM salvicine.

Downloaded from molpharm.aspetjournals.org by guest on December 1, 2012

MOL PHARM
MOLECULAR PHARMACOLOGY
aspet

but did not change the growth rate of salvicine-treated JN394top2-4 at 35°C (Fig. 5C). This result clearly showed that Topo II was one target of salvicine-induced ROS, although it is unclear which ROS might elicit DNA DSBs and the subsequent growth inhibition.

ROS Contribute to the Down-Regulation of DNA-PKcs Protein Levels. Salvicine-induced DSBs may be caused by the enhancement of DNA damage and/or the inhibition of DNA damage repair. There are two distinct but complementary mechanisms for DNA DSB repair—nonhomologous end joining (NHEJ) and homologous recombination (HR)—both of which are complicated cascades involving various repair proteins. Three protein complexes, DNA-PK, Mre11-Rad50-Nbs1, and Rad51, have thus far been identified as playing important roles in these two repair mechanisms (Khanna and Jackson, 2001). NHEJ is the predominant pathway for DSB repair (including Topo II-mediated DNA damage repair) in mammals (Adachi et al., 2003). DNA-PK, which is composed of a large catalytic subunit (DNA-PKcs) of approximately 450 kDa and two smaller Ku subunits (Ku70 and Ku86), is a critical component of this pathway (Smith and Jackson, 1999; Pastwa and Blasiak, 2003). To ascertain the effect of salvicine on this DNA DSB repair pathway after salvicine-induced DNA damage, we investigated the effect of salvicine on Ku70, Ku86, and DNA-PKcs protein levels. Although the protein levels of Ku70 and Ku86 remained unaltered, the levels of DNA-PKcs were reduced in a concentration-dependent manner in salvicine-treated MCF-7 cells (Fig. 6, A and B). Moreover, NAC pretreatment attenuated the salvicine-induced reduction of DNA-PKcs, indicating that ROS are involved in this process (Fig. 6B). To assess the importance of the HR pathway, we examined the effects of salvicine on expression of Mre11, which is implicated in both HR and NHEJ, and Rad51, which is a key component in the HR pathway (Kowalczykowski, 2000). The protein levels of Mre11 and Rad51 were unchanged after salvicine exposure (Fig. 6A), suggesting that salvicine and/or salvicine-induced ROS mainly act on the NHEJ repair pathway, although we cannot completely exclude its influence on the HR pathway.

ROS Are Implicated in the Inhibition of DNA-PK Activity. DNA-PK is a member of the phosphatidyl 3-kinase–like family and possesses protein serine/threonine kinase activities that are vital for NHEJ repair (Smith and Jackson, 1999; Pastwa and Blasiak, 2003). Thus, we further investigated the impact of salvicine on DNA-PK activity. MCF-7 cells were exposed to gradient concentrations of salvicine for 4 h; the DNA-PK activity was inhibited in a concentration-dependent manner. The inhibition rates increased from 9.83 to 44.39% as the concentration of salvicine increased from 10 to 40 μM (Fig. 7A). NAC pretreatment effectively abrogated the salvicine-induced inhibition of DNA-PK kinase activity, indicating that ROS contributed to this process. In view of the impact of salvicine on DNA-PK subunit expression in MCF-7 cells, these data seemed to indicate that the salvicine-induced ROS led to the depression of DNA-PK enzyme activity partially via reducing the level of DNA-PKcs protein.

Treatment with Salvicine Does Not Alter the Subcellular Distribution of DNA-PK Subunits. Given the important role of Ku70, Ku86, and DNA-PKcs in regulating the kinase activity of DNA-PK, we examined the subcellular distribution of DNA-PK subunits after salvicine treatment. MCF-7 cells were fixed and stained with specific antibodies against these proteins. As shown in Fig. 8, there was no significant alteration in the subcellular distribution of the DNA-PK subunits, which were primarily localized in the nuclei (marked by DAPI staining) of both salvicine-treated MCF-7 cells and control cells. This result demonstrated that the inhibition of DNA-PK activity was not caused by relocalization of DNA-PK subunits.

ROS Partially Mediate Salvicine-Induced Apoptosis and Growth Inhibition. To further evaluate the contribu-

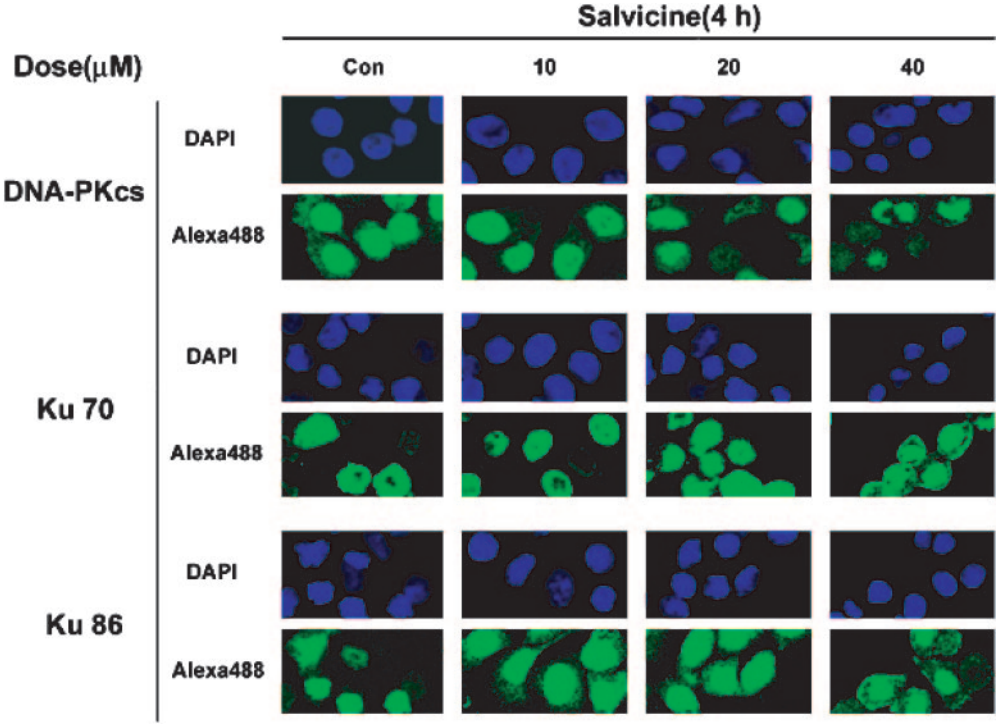

Fig. 8. Effects of salvicine on the subcellular distribution of DNA-PK subunits. Cells were treated as indicated, fixed, stained with DAPI and Alexa488-labeled secondary antibodies, and examined by confocal microscopy (oil, 63×). The experiments were repeated three times.

Downloaded from molpharm.aspetjournals.org by guest on December 1, 2012

MOL PHARM
MOLECULAR PHARMACOLOGY
aspet

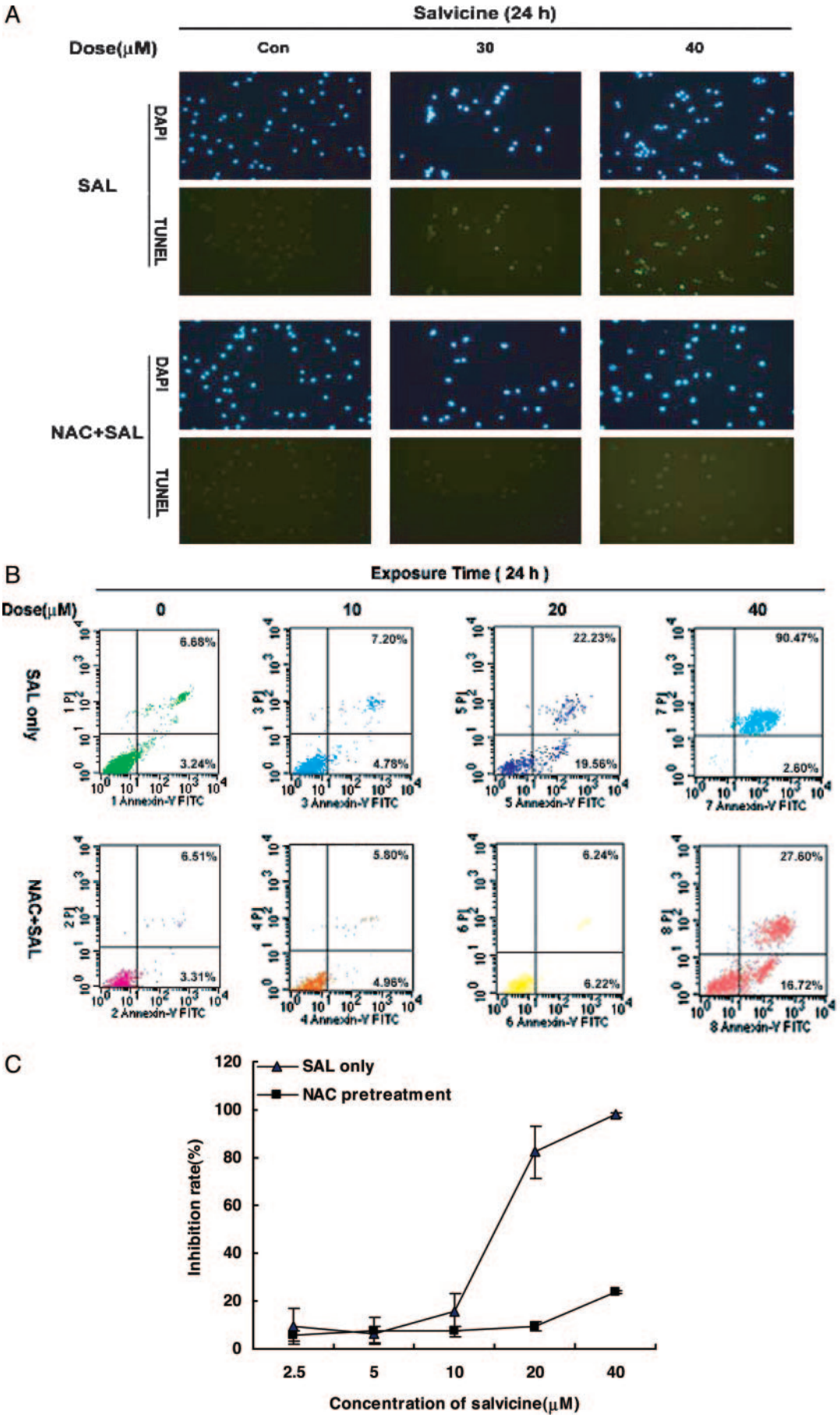

Downloaded from molpharm.aspetjournals.org by guest on December 1, 2012

MOL PHARM

MOLECULAR PHARMACOLOGY

tion of salvicine-induced ROS to the biological consequences of salvicine treatment, we determined the effect of NAC pretreatment on salvicine-induced apoptosis and growth inhibition in MCF-7 cells. We used two independent methods to investigate the effects of NAC pretreatment on salvicine-induced apoptosis in MCF-7 cells. TUNEL staining revealed that exposure of MCF-7 cells to salvicine for 24 h led to concentration-dependent apoptosis regardless of NAC pretreatment (Fig. 9A), but the degree of apoptosis was much lower in the NAC-pretreated group. The results of flow cytometric analysis of cells double stained with Annexin V-FITC and propidium iodide were consistent with the TUNEL data (Fig. 9B). These results were further validated by the effect of NAC pretreatment on salvicine cytotoxicity in MCF-7 cells. In cells treated with 40 μM salvicine, NAC pretreatment reduced the growth inhibition rate from 97.91 to 23.54% (Fig. 9C). These results collectively indicated that salvicine-induced ROS were the critical mediators in salvicine-induced tumor cell killing.

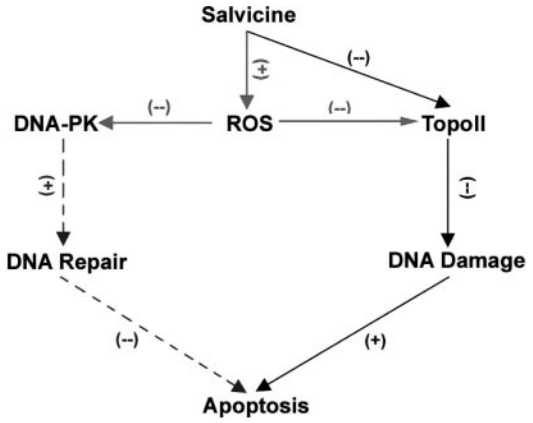

Fig. 10. Salvicine elicits apoptosis through the dual modulation of DNA damage and related repair pathways. On one hand, salvicine induced DNA damage by inhibiting Topo II through direct effect and/or the possible oxidative modification on the key residues of Topo II by salvicine-induced ROS. On the other hand, salvicine disrupts the corresponding repair mechanism by inhibiting the activities of DNA-PK through the ROS-related down-regulation of the protein level of DNA-PKcs. +, stimulate; −, inhibit.

Discussion

ROS have been studied extensively in terms of their effects on various cellular processes. Multiple antitumor therapies, including chemotherapeutic drugs and irradiation, can stimulate ROS production in tumor cells, perhaps contributing to their antitumor activities. Thus, a more profound understanding of the molecular mechanisms of ROS in tumor cells may foster new antitumor strategies. In this study, we showed that salvicine, a novel Topo II inhibitor currently under phase I clinical trial, stimulated intracellular ROS production and subsequently elicited notable DNA DSBs in human breast carcinoma MCF-7 cells. The addition of NAC effectively decreased salvicine-induced ROS enhancement and the subsequent DNA DSBs, establishing a possible causal correlation between the two phenomena. Both the heat-induced reversal of DNA DSBs and the NAC-mediated attenuation of Topo II-DNA–cleavable complexes formation and growth inhibition in salvicine-treated JN394top2-4 indicated that Topo II is one target of the salvicine-induced ROS. These data also suggest that the induced ROS may act as signaling molecules rather than directly breaking the DNA duplex. Several previous studies have identified various mechanisms involved in the activation of Topo II-mediated DNA cleavage, including DNA structural modification, enzyme modification, acidic pH environment, and oxidative stress (Zechiedrich et al., 1989; Kingma and Osheroff, 1997; Li et al., 1999; Wang et al., 2001). The thiol-containing cysteine residue, generally as a catalytic element in the active domains of enzymatic proteins, can be oxidatively modified by ROS, thus leading to enzyme inactivation (Michiels et al., 2002). H_2O_2 (a well-known ROS) was shown to activate Topo II-mediated DNA breaks in vitro, probably through oxidation of the critical thiol group(s) on Topo II (Li et al., 1999). Therefore, although it remains to be clarified exactly how ROS regulate Topo II, we can reasonably infer that ROS mediate the DNA damage observed in our system through oxidative modification of key cysteine residues on Topo II. Our results provide novel evidence that antineoplastic-induced ROS attack Topo II to generate DNA DSBs.

When examining the impact of salvicine on the DNA damage-repair pathways, we unexpectedly observed that salvicine repressed DNA-PK kinase activity. This result is interesting because DNA DSBs induced by antitumor agents will generally activate, not repress, the DNA damage-repair system. DNA-PK, an essential component in the NHEJ repair pathway, is a serine/threonine protein kinase whose catalytic activity is triggered upon association with DNA ends (Smith and Jackson, 1999; Pastwa and Blasiak, 2003). A recent study showed that treatment of the human head and neck squamous carcinoma cell line A253 with the Topo I inhibitor SN-38 (an active metabolite of irinotecan) resulted in biphasic DSBs and activation of three DSB repair protein complexes, DNA-PK, Mre11-Rad50-Nbs1, and BRCA1 (Wu et al., 2002). Bleomycin, calicheamicin, and ionizing radiation also activate DNA-PK to levels matching the kinase activation obtained with simple restriction endonuclease-induced DSBs (Martensson et al., 2003). However, in the current study, salvicine (a Topo II poison) inhibited DNA-PK activity even though the DNA ends resulting from the salvicine-induced DSBs should theoretically form appropriate inducers for DNA-PK activation. One mechanism may be responsible for such inhibition. That is the salvicine-induced down-regulation of a catalytic subunit of DNA-PK, DNA-PKcs, which may counteract the DSB-induced DNA-PK activation. We found that NAC pretreatment reversed the down-regulation of DNA-PKcs protein levels and the inhibition of DNA-PK activity. These results suggest that salvicine-induced ROS also play an important role in the inhibition of DNA repair by salvicine. Although ROS have been reported recently to affect the repair of DNA DSBs in tumor drug resistance by altering DNA-PK activity (Boldogh et al., 2003), the precise relation-

Fig. 9. Effect of NAC on salvicine-induced apoptosis and cytotoxicity. MCF-7 cells were treated with various concentrations of salvicine for 24 h and harvested for apoptosis detection. A, DAPI and TUNEL staining. B, density plot of flow cytometric analysis of Annexin V-FITC and PI double-stained cells. Cells staining Annexin V^+/PI^- and Annexin V^+/PI^+ represent the early and late apoptotic events, respectively. C, growth inhibition was evaluated by SRB dye assay. The data were expressed as mean ± S.D. (n = 3).

Downloaded from molpharm.aspetjournals.org by guest on December 1, 2012

ship between ROS and DNA-PK is not yet fully understood. Our data thus offer the first line of experimental evidence for the potential role of ROS in the regulation of DNA-PKcs.

The fact that NAC attenuated salvicine-induced apoptosis and cytotoxicity in MCF-7 cells is noteworthy because it provides additional evidence for the causal role of ROS in salvicine-induced tumor cell death. These data indicate that salvicine-induced ROS cause DNA DSBs and the final biological effects by disrupting both Topo II and the NHEJ repair pathway (via inactivation of DNA-PK). This novel mode of ROS action sheds new lights on the complex biological behavior of ROS. The finding that salvicine induces ROS also provides an important new insight into the molecular mechanisms of this compound. Together with our previous studies, these data allow us to propose the following conclusions (Fig. 10): 1) salvicine disrupts the balance of cellular DNA integrity by enhancing DNA damage and inhibiting DNA damage repair; 2) apart from its direct actions, salvicine generates ROS, which may act as signaling molecules; and 3) salvicine-induced ROS act on Topo II and DNA-PK, contributing to the comprehensive biological consequences of salvicine, including DNA DSBs, apoptosis, and cytotoxicity in tumor cells.

In summary, we herein demonstrated that salvicine itself, together with salvicine-induced ROS, simultaneously disrupt both Topo II and DNA-PK, leading to the modulation of two aspects of DNA damage and repair and accounting at least in part for the antitumor effects of salvicine. These findings suggest that the existing DNA-damaging anticancer treatments of ionizing radiation and cytotoxic drugs may be improved by specific targeting of key DNA repair proteins.

References

Adachi N, Suzuki H, Iiizumi S, and Koyama H (2003) Hypersensitivity of nonhomologous DNA end-joining mutants to VP-16 and ICRF-193: implications for the repair of topoisomerase II-mediated DNA damage. *J Biol Chem* **278:**35897–35902.

Binaschi M, Farinosi R, Austin CA, Fisher LM, Zunino F, and Capranico G (1998) Human DNA topoisomerase IIalpha-dependent DNA cleavage and yeast cell killing by anthracycline analogues. *Cancer Res* **58:**1886–1892.

Boldogh I, Roy G, Lee MS, Bacsi A, Hazra TK, Bhakat KK, Das GC, and Mitra S (2003) Reduced DNA double strand breaks in chlorambucil resistant cells are related to high DNA-PKcs activity and low oxidative stress. *Toxicology* **193:**137–152.

Dai J, Weinberg RS, Waxman S, and Jing Y (1999) Malignant cells can be sensitized to undergo growth inhibition and apoptosis by arsenic trioxide through modulation of the glutathione redox system. *Blood* **93:**268–277.

Eriksson A, Yachnin J, Lewensohn R, and Nilsson A (2001) DNA-dependent protein kinase is inhibited by trifluoperazine. *Biochem Biophys Res Commun* **283:**726–731.

Haddad JJ (2004) Redox and oxidant-mediated regulation of apoptosis signaling pathways: immuno-pharmaco-redox conception of oxidative siege versus cell death commitment. *Int Immunopharmacol* **4:**475–493.

Hammonds TR, Maxwell A, and Jenkins JR (1998) Use of a rapid throughput in vivo screen to investigate inhibitors of eukaryotic topoisomerase II enzymes. *Antimicrob Agents Chemother* **42:**889–894.

Hancock JT, Desikan R, and Neill SJ (2001) Role of reactive oxygen species in cell signalling pathways. *Biochem Soc Trans* **29:**345–350.

Higuchi Y (2003) Chromosomal DNA fragmentation in apoptosis and necrosis induced by oxidative stress. *Biochem Pharmacol* **66:**1527–1535.

Hsiang YH and Liu LF (1989) Evidence for the reversibility of cellular DNA lesion induced by mammalian topoisomerase II poisons. *J Biol Chem* **264:**9713–9715.

Jabs T (1999) Reactive oxygen intermediates as mediators of programmed cell death in plants and animals. *Biochem Pharmacol* **57:**231–245.

Kamata H and Hirata H (1999) Redox regulation of cellular signalling. *Cell Signal* **11:**1–14.

Khanna KK and Jackson SP (2001) DNA double-strand breaks: signaling, repair and the cancer connection. *Nat Genet* **27:**247–254.

Kingma PS and Osheroff N (1997) Spontaneous DNA damage stimulates topoisomerase II-mediated DNA cleavage. *J Biol Chem* **272:**7488–7493.

Kotamraju S, Kalivendi SV, Konorev E, Chitambar CR, Joseph J, and Kalyanaraman B (2004) Oxidant-induced iron signaling in doxorubicin-mediated apoptosis. *Methods Enzymol* **378:**362–382.

Kowalczykowski SC (2000) Initiation of genetic recombination and recombination-dependent replication. *Trends Biochem Sci* **25:**156–165.

LeBel CP, Ischiropoulos H, and Bondy SC (1992) Evaluation of the probe 2′,7′-dichlorofluorescin as an indicator of reactive oxygen species formation and oxidative stress. *Chem Res Toxicol* **5:**227–231.

Li TK, Chen AY, Yu C, Mao Y, Wang H, and Liu LF (1999) Activation of topoisomerase II-mediated excision of chromosomal DNA loops during oxidative stress. *Genes Dev* **13:**1553–1560.

Liu WJ, Jiang JF, Xiao D, and Ding J (2002) Down-regulation of telomerase activity via protein phosphatase 2A activation in salvicine-induced human leukemia HL-60 cell apoptosis. *Biochem Pharmacol* **64:**1677–1687.

Lu HR, Meng LH, Huang M, Zhu H, Miao ZH, and Ding J (2005) DNA damage, C-Myc suppression and apoptosis induced by the novel topoisomerase II inhibitor, salvicine, in human breast cancer MCF-7 Cells. *Cancer Chemother Pharmacol* **55:**286–294.

Martensson S, Nygren J, Osheroff N, and Hammarsten O (2003) Activation of the DNA-dependent protein kinase by drug-induced and radiation-induced DNA strand breaks. *Radiat Res* **160:**291–301.

Meng LH, He XX, Zhang JS, and Ding J (2001a) DNA topoisomerase II as the primary cellular target for salvicine in *Saccharomyces cerevisiae*. *Acta Pharmacol Sin* **22:**741–746.

Meng LH, Zhang JS, and Ding J (2001b) Salvicine, a novel DNA topoisomerase II inhibitor, exerting its effects by trapping enzyme-DNA cleavage complexes. *Biochem Pharmacol* **62:**733–741.

Miao ZH and Ding J (2003) Transcription factor C-Jun activation represses Mdr-1 gene expression. *Cancer Res* **63:**4527–4532.

Miao ZH, Tang T, Zhang YX, Zhang JS, and Ding J (2003) Cytotoxicity, apoptosis induction and downregulation of MDR-1 expression by the anti-topoisomerase II agent, salvicine, in multidrug-resistant tumor cells. *Int J Cancer* **106:**108–115.

Michiels C, Minet E, Mottet D, and Raes M (2002) Regulation of gene expression by oxygen: NF-KappaB and HIF-1, two extremes. *Free Radic Biol Med* **33:**1231–1242.

Minotti G, Ronchi R, Salvatorelli E, Menna P, and Cairo G (2001) Doxorubicin irreversibly inactivates iron regulatory proteins 1 and 2 in cardiomyocytes: evidence for distinct metabolic pathways and implications for iron-mediated cardiotoxicity of antitumor therapy. *Cancer Res* **61:**8422–8428.

Olive PL, Banath JP, and Durand RE (1990) Heterogeneity in radiation-induced DNA damage and repair in tumor and normal cells measured using the "Comet" assay. *Radiat Res* **122:**86–94.

Pastwa E and Blasiak J (2003) Non-homologous DNA end joining. *Acta Biochim Pol* **50:**891–908.

Qing C, Jiang C, Zhang JS, and Ding J (2001) Induction of apoptosis in human leukemia K-562 and gastric carcinoma SGC-7901 cells by salvicine, a novel anticancer compound. *Anticancer Drugs* **12:**51–56.

Qing C, Zhang JS, and Ding J (1999) In vitro cytotoxicity of salvicine, a novel diterpenoid quinone. *Acta Pharmacol Sin* **20:**297–302.

Shiah SG, Chuang SE, Chau YP, Shen SC, and Kuo ML (1999) Activation of C-Jun NH2-terminal kinase and subsequent CPP32/Yama during topoisomerase inhibitor beta-lapachone-induced apoptosis through an oxidation-dependent pathway. *Cancer Res* **59:**391–398.

Sidoti-de Fraisse C, Rincheval V, Risler Y, Mignotte B, and Vayssiere JL (1998) TNF-alpha activates at least two apoptotic signaling cascades. *Oncogene* **17:**1639–1651.

Smith GC and Jackson SP (1999) The DNA-dependent protein kinase. *Genes Dev* **13:**916–934.

Wang H, Mao Y, Chen AY, Zhou N, LaVoie EJ, and Liu LF (2001) Stimulation of topoisomerase II-mediated DNA damage via a mechanism involving protein thiolation. *Biochemistry* **40:**3316–3323.

Willmore E, Frank AJ, Padget K, Tilby MJ, and Austin CA (1998) Etoposide targets topoisomerase IIα and IIβ in leukemic cells: isoform-specific cleavable complexes visualized and quantified in situ by a novel immunofluorescence technique. *Mol Pharmacol* **54:**78–85.

Wu J, Yin MB, Hapke G, Toth K, and Rustum YM (2002) Induction of biphasic DNA double strand breaks and activation of multiple repair protein complexes by DNA topoisomerase I drug 7-ethyl-10-hydroxy-camptothecin. *Mol Pharmacol* **61:**742–748.

Yi J, Yang J, He R, Gao F, Sang H, Tang X, and Ye RD (2004) Emodin enhances arsenic trioxide-induced apoptosis via generation of reactive oxygen species and inhibition of survival signaling. *Cancer Res* **64:**108–116.

Zafarullah M, Li WQ, Sylvester J, and Ahmad M (2003) Molecular mechanisms of N-acetylcysteine actions. *Cell Mol Life Sci* **60:**6–20.

Zechiedrich EL, Christiansen K, Andersen AH, Westergaard O, and Osheroff N (1989) Double-stranded DNA cleavage/religation reaction of eukaryotic topoisomerase II: evidence for a nicked DNA intermediate. *Biochemistry* **28:**6229–6236.

Zhang JS, Ding J, Tang QM, Li M, Zhao M, Lu LJ, Chen LJ, and Yuan ST (1999) Synthesis and antitumour activity of novel diterpenequinone salvicine and the analogs. *Bioorg Med Chem Lett* **9:**2731–2736.

Address correspondence to: Dr. Jian Ding, Division of Anti-tumor Pharmacology, State Key Laboratory of Drug Research, Shanghai Institute of *Materia Medica*, Shanghai Institutes for Biological Sciences, Chinese Academy of Sciences, Shanghai 201203, Peoples Republic of China. E-mail: jding@mail.shcnc.ac.cn

MOL PHARM
MOLECULAR PHARMACOLOGY
aspet
Downloaded from molpharm.aspetjournals.org by guest on December 1, 2012